**The EMBO Journal** Vol.16 No.12 pp.3386–3395, 1997

# Crystal structure of human glyoxalase I—evidence for gene duplication and 3D domain swapping

**Alexander D.Cameron, Birgit Olin[1], Marianne Ridderström[1], Bengt Mannervik[1,2] and T.Alwyn Jones[2]**

Department of Molecular Biology, Uppsala University, Biomedical Center, Box 590, S-751 24, Uppsala and [1]Department of Biochemistry, Uppsala University, Biomedical Center, Box 576, S-751 23, Uppsala, Sweden

[2]Corresponding author

**The zinc metalloenzyme glyoxalase I catalyses the glutathione-dependent inactivation of toxic methylglyoxal. The structure of the dimeric human enzyme in complex with *S*-benzyl-glutathione has been determined by multiple isomorphous replacement (MIR) and refined at 2.2 Å resolution. Each monomer consists of two domains. Despite only low sequence homology between them, these domains are structurally equivalent and appear to have arisen by a gene duplication. On the other hand, there is no structural homology to the 'glutathione binding domain' found in other glutathione-linked proteins. 3D domain swapping of the N- and C-terminal domains has resulted in the active site being situated in the dimer interface, with the inhibitor and essential zinc ion interacting with side chains from both subunits. Two structurally equivalent residues from each domain contribute to a square pyramidal coordination of the zinc ion, rarely seen in zinc enzymes. Comparison of glyoxalase I with other known structures shows the enzyme to belong to a new structural family which includes the $Fe^{2+}$-dependent dihydroxybiphenyl dioxygenase and the bleomycin resistance protein. This structural family appears to allow members to form with or without domain swapping.**

*Keywords*: gene duplication/glutathione/glyoxalase I/3D domain swapping/zinc coordination

## Introduction

The glyoxalase system catalyses the conversion of 2-oxoaldehydes into the corresponding 2-hydroxycarboxylic acids using glutathione as coenzyme. It consists of two enzymes, glyoxalase I and glyoxalase II, and is found in organisms throughout the evolutionary scale (Mannervik, 1980; Thornalley, 1990). Since 2-oxoaldehydes are cytostatic at low concentrations and cytotoxic at high concentrations, the system is thought to be involved in detoxication. An important endogenous substrate appears to be methylglyoxal which is generated in a side reaction of the triose phosphate isomerase (TIM) reaction (Richard, 1991). In addition to its role as a detoxication system, it has been suggested that the glyoxalase system is involved in the regulation of cellular growth (Szent-Györgyi, 1965) and in the assembly of microtubules (Gillespie, 1979). Furthermore, modulation of its activity may be relevant to both cancer and diabetes. Glyoxalase I has been targeted for the development of novel anti-tumour, anti-protozoal and anti-bacterial agents that by inhibition would raise methylglyoxal concentrations to toxic levels (Thornalley, 1993).

Glyoxalase I (EC 4.4.1.5) catalyses the isomerization of the thiohemiacetal of glutathione (GSH) and a 2-oxoaldehyde into the thiolester of GSH and the corresponding 2-hydroxycarboxylic acid. The substrate of the reaction, the thiohemiacetal, is formed non-enzymatically. Glyoxalase II then hydrolyses the thiolester to produce GSH and a free 2-hydroxycarboxylic acid. Human glyoxalase I is a dimer of 43 kDa containing 183 amino acid residues per monomer. It has been cloned and heterologously expressed in *Escherichia coli* (Kim *et al.*, 1993; Ranganathan *et al.*, 1993; Ridderström and Mannervik, 1996a). Metal analysis of both recombinant protein and protein purified from human erythrocytes shows $Zn^{2+}$ ions to be present in a stoichiometric ratio of 1.0 mol $Zn^{2+}$/1.0 mol of subunit, with other metal ions present only at much lower concentrations (Aronsson *et al.*, 1978; Ridderström and Mannervik, 1996a). Although a metal ion is essential for catalysis, the enzyme is unusual in that replacement of the native zinc ion with $Mg^{2+}$ restores full catalytic activity. Other divalent cations yield an active but generally slightly impaired enzyme (Sellin *et al.*, 1983; Sellin and Mannervik, 1984). It has been reported, however, that there is no activity on replacement of the zinc with ferrous ions, at least under aerobic conditions (Uotila and Koivusalo, 1975).

## Results and discussion

The structure of recombinant human glyoxalase I has been solved using a combination of multiple isomorphous replacement (MIR) and 4-fold molecular averaging, and refined to a resolution of 2.2 Å while maintaining strict non-crystallographic symmetry (NCS) constraints between molecules. The crystallographic R-factor based on all data between 7.5 and 2.2 Å is 21.1%, and the corresponding R-free 23.4%, for a model containing residues 8–183, an *S*-benzyl-glutathione inhibitor, one zinc ion and 90 water molecules per monomer. The first seven residues were not located in the electron density.

### *Overall structure*

The monomer is built up from two domains (residues 31–104 and 124–183), linked by a 20 residue connection and preceded by a long N-terminal arm. This arm does not interact with either domain (Figure 1A). Within each domain there is a common motif of βαββββ topology, with strands 1–4–3–2 abutting one another to form a mixed β sheet. In the first domain, there is an additional α helix

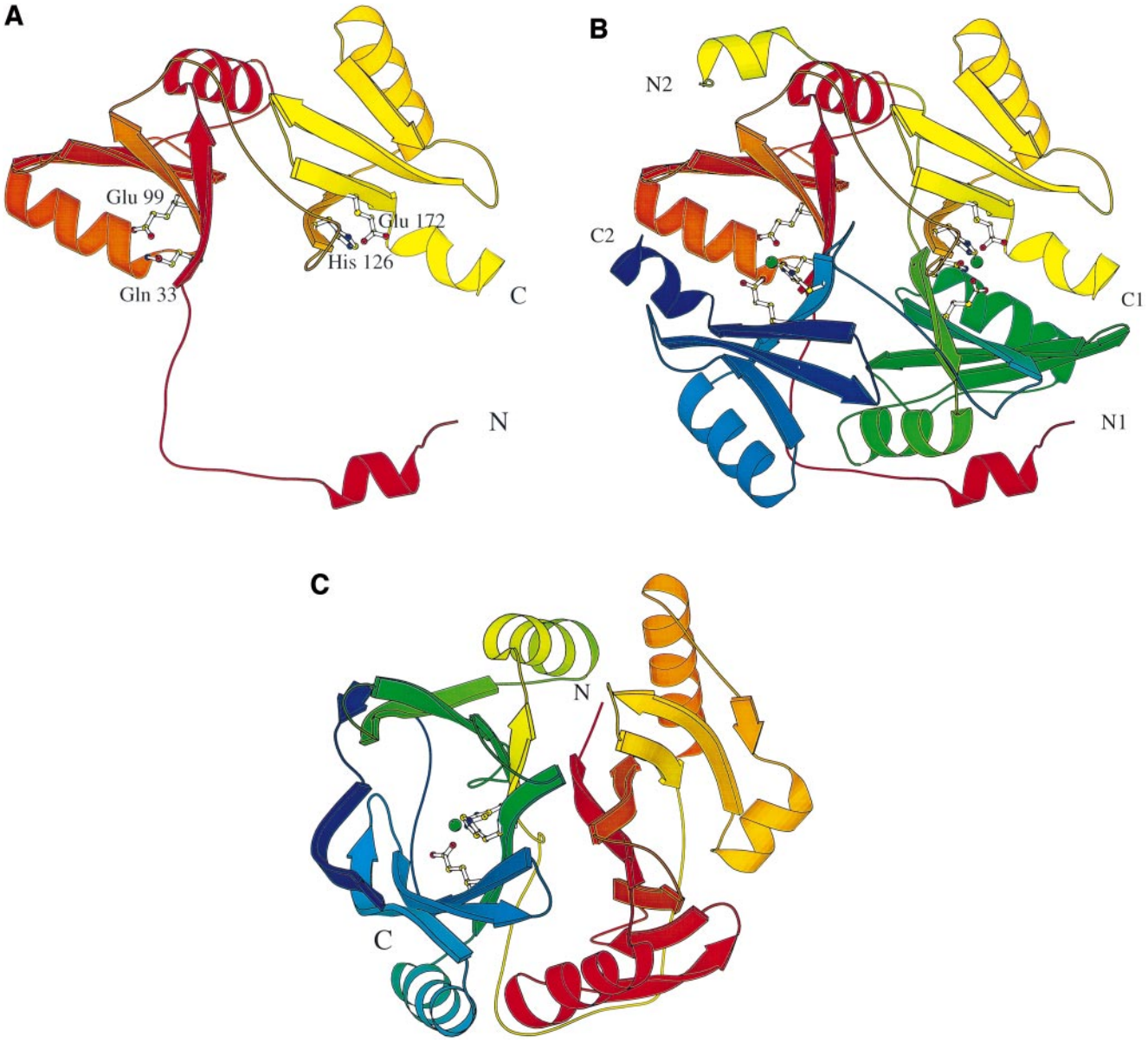


**Fig. 1.** Schematic representation of glyoxalase I. (**A**) Monomer; (**B**) dimer. The dimer has been colour ramped according to residue number, starting with red at the N-terminus of one molecule, passing through yellow at the C-terminus of that molecule and finishing with blue at the C-terminus of the other monomer. The zinc and its coordinating residues are shown in a ball and stick representation with the zinc coloured green. The active site is situated in a barrel which is formed only on dimerization. Residue 114 is situated at the end of the red/yellow domain and residue 123 at the beginning of the blue/green domain (see the text). Prepared using MOLSCRIPT (Kraulis, 1991) modified by R.Esnouf (Oxford University, unpublished). (**C**) A similar view of the dihydroxybiphenyl dioxygenase (DHBD) enzyme (Han *et al.*, 1995) after superposition on the human glyoxalase I enzyme. Again the molecule has been colour ramped according to residue number, starting with red at the N-terminus and finishing with blue at the C-terminus. Despite having only 14% sequence identity (using the structures to align the sequences), 79 Cα pairs from the C-terminal domains of this enzyme (blue and green) can be aligned on glyoxalase I with an r.m.s.d. of 2 Å. The colouring scheme clearly shows that the suggested domain swapping in glyoxalase I is not present in DHBD. The ferrous iron seen in DHBD is situated in a similar position to one of the zincs in glyoxalase I. The residues coordinating the iron are structurally equivalent to those binding the zinc.

between strands 3 and 4 such that the full topology of the domain is βαββαβ. In contrast, the topology of the complete C-terminal domain is βαββββα. The similarity of the domains means that 42 out of a possible 59 Cα pairs can be superimposed with a root mean square deviation (r.m.s.d.) of 1.8 Å (see Figure 2 and Materials and methods).

The active enzyme is a dimer of identical subunits. Within the limits of the crystallographic experiment, the monomers making up the dimer are related by a pure 2-fold axis, with no translational symmetry. In the dimer, the first strand of the first domain of one monomer interacts in an anti-parallel fashion with the first strand of the second domain of the opposing monomer so that an eight-stranded β sheet is formed. This sheet combines with the extra helix of domain 1 and the C-terminal helix of domain 2 to form a barrel containing the active site at the dimer interface (see Figure 1B). The Cα atoms of residue 114, which is situated at the C-terminus of the first domain of one monomer, and residue 123, at the N-terminus of the second domain of the opposing monomer, are only 4.7 Å apart. It is, therefore, easy to visualize a protein which is

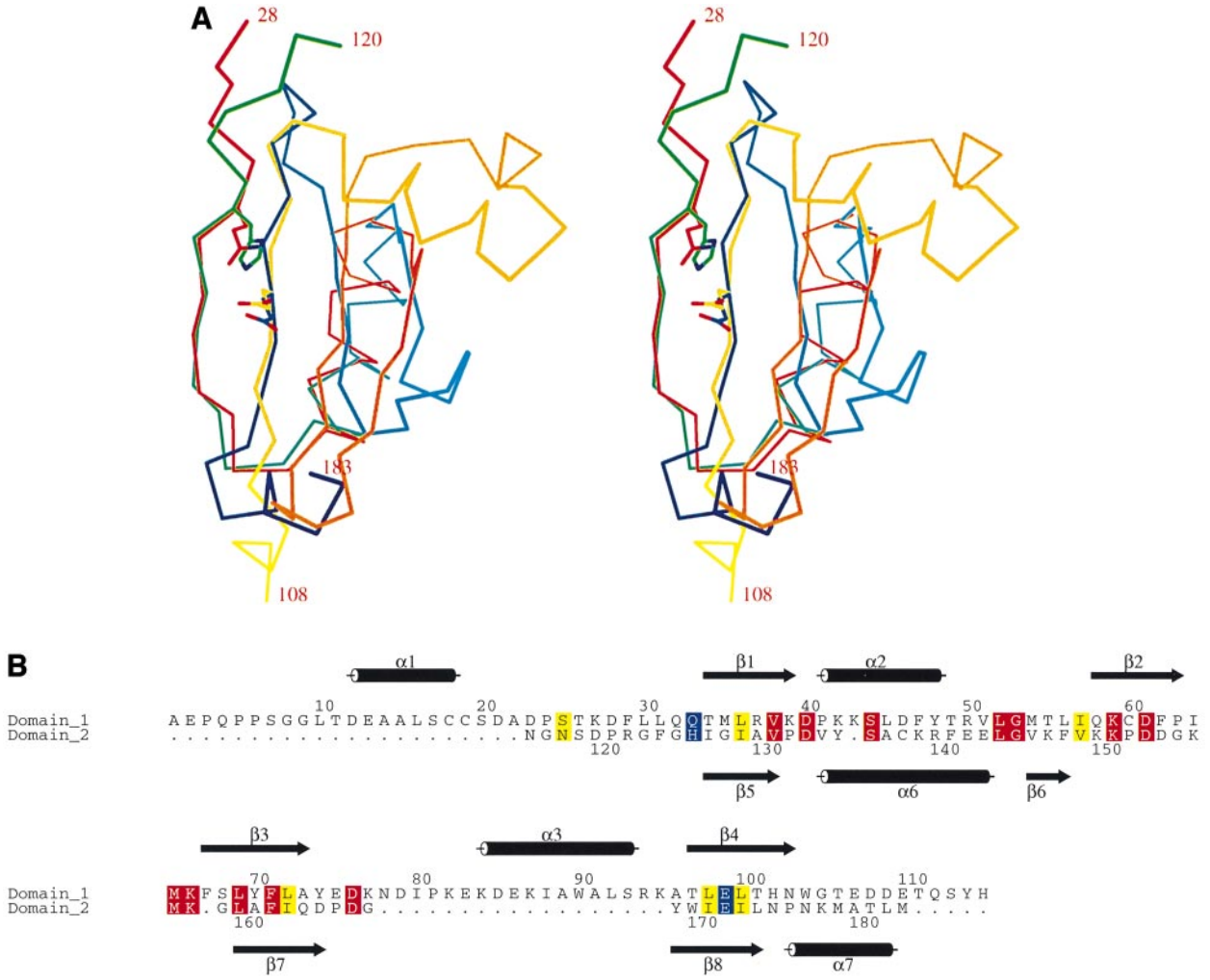


**Fig. 2.** (**A**) Stereo diagram showing the superposition of domain 1 on domain 2. The figure has been colour ramped according to residue number as in Figure 1. The zinc ligands are shown with carbon atoms coloured according to the backbone. (**B**) Sequence alignment of the two domains. The sequences were aligned based on the structural superposition. The residues binding the metal have been coloured dark blue, identical residues red and conserved residues yellow. Secondary structure was defined using the YASSPA algorithm implemented in O. The figure was prepared using the program ALSCRIPT (Barton, 1993).

essentially the same as that shown in Figure 1B, but where the red and blue domains are covalently linked to form one monomer, and the yellow and green domains are linked to form the other. The active site would then be completely contained within one monomer. Eisenberg and co-workers have recently pointed out that in some proteins which have both monomeric and oligomeric forms, a domain in the monomer may be replaced by an equivalent domain from another subunit in the oligomeric form of the protein (Bennett *et al.*, 1995). This, so-called, 3D domain swapping is the situation we observe in glyoxalase I.

### *Zinc binding site*

The active site zinc ion is situated in the middle of the barrel and is coordinated by four protein residues and one water molecule (see Figure 3). Each domain contributes two residues to zinc binding. Upon overlaying the two domains based on a least squares fit of their respective Cα atoms, the two zinc ligands from domain 1 (Gln 33 and Glu 99) superimpose almost exactly on the pair from domain 2 (His 126 and Glu 172; see Figure 2A). The coordination geometry is square pyramidal, i.e. essentially octahedral with one ligand absent. The distortion from a true square pyramid is rather small. The zinc lies below the plane of the square pyramid, defined by the OE1 atoms of Gln 33, Glu 99 and Glu 172 and the water molecule. It is displaced ~0.5 Å towards His 126, the axial ligand. The zinc ligand distances are between 2.0 and 2.1 Å, and the angles subtended by the zinc and the equatorial ligands lie in a range between 83 and 92°. Both carboxylates are bound to the zinc via their *syn*-oriented lone electron pair. With respect to the planes of the individual residues, the zinc lies only ~0.2° out of the planes of His 126 and Gln 33, respectively, but further from the planes of the carboxylates (0.5 Å from Glu 99 and 1.0 Å from Glu 172), perhaps indicating that the carboxylate–zinc interactions are weaker. The functional group of Glu 99 also has a slightly higher average B-factor (25 $Å^2$) than the functional groups of the other ligands (Glu 172, 19 $Å^2$; Gln 33, 16 $Å^2$; His 126, 10 $Å^2$). The B-factor of the zinc ion, 19 $Å^2$, is comparable with the average B-factor of the protein, 23 $Å^2$. The ligand arrangement is in general agreement with EXAFS and

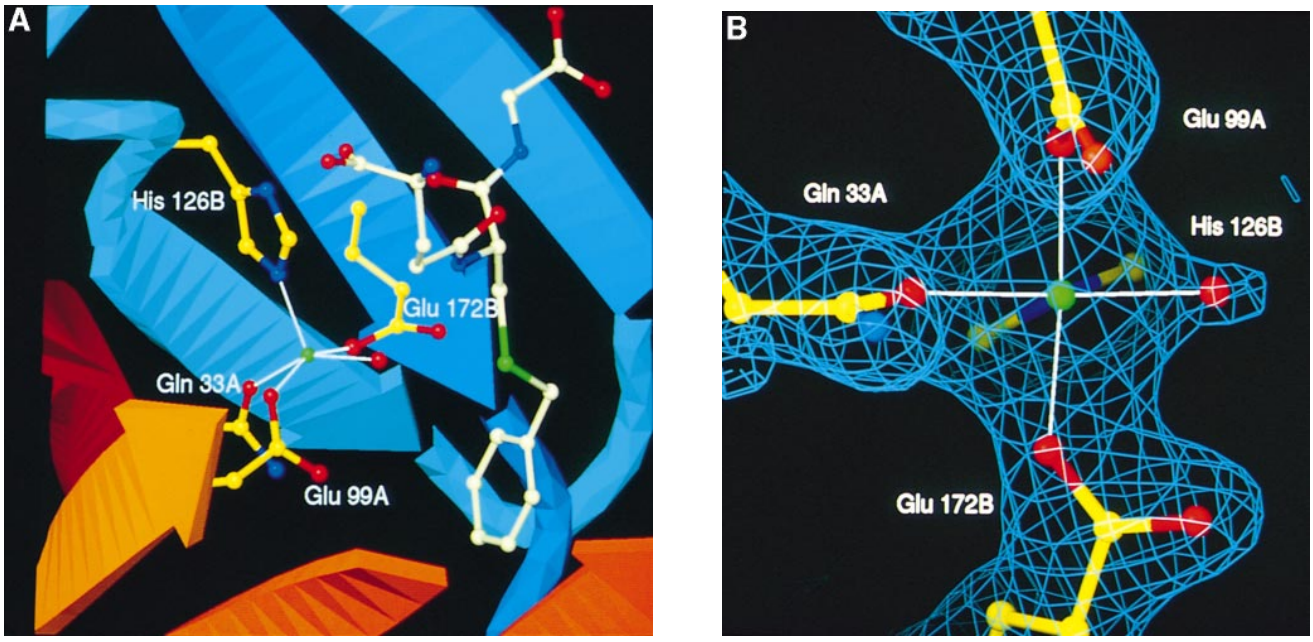


**Fig. 3.** Two views of the zinc binding site. The two central β strands in the foreground have been curtailed to expose the zinc binding site. The schematic representation of the backbone has been coloured as in Figure 1. Carbon atoms of the protein residues have been coloured yellow and those of the *S*-benzyl-glutathione cream. The zinc, the zinc-bound water and the sulfur atom of the glutathione are co-linear. The density shown in (**B**) is from a map calculated using phases derived from the final structure and then subjected to 10 cycles of averaging (contoured at 1σ). The octahedral arrangement of zinc ligands can clearly be seen in this view. The distances between the zinc ion and Gln 33 OE1, Glu 99 OE1, His 126 NE2, Glu 172 OE1 and the water are 2.0, 2.0, 2.1, 2.0 and 2.1 Å, respectively. No distance or angle restraints were applied to the coordination geometry during refinement. The figures were prepared in O (Jones and Kjeldgaard, 1991; Jones *et al.*, 1991).

EPR experiments on glyoxalase I that indicate a distorted octahedral coordination of the metal (Sellin *et al.*, 1983, 1987; Garcia-Iniguez *et al.*, 1984; Sellin and Mannervik, 1984). The sixth ligand, which would complete the octahedral arrangement, is not present in our electron density. Proton relaxation studies on the $Mn^{2+}$-substituted enzyme have shown that there are two rapidly exchanging water molecules in the apo-enzyme, whereas only one is detectable after the addition of either *S*-(*p*-bromobenzyl) glutathione or *S*-(D-lactoyl) glutathione (Sellin *et al.*, 1982a,b).

In small molecule complexes, zinc displays coordination numbers of 4, 5 or 6, with a coordination number of 4 being almost twice as common as 6, and 5 less common (Bock *et al.*, 1995). However, zinc ions in protein structures generally have a tetrahedral arrangement of ligands (Christianson, 1991) and, to the best of our knowledge, only two proteins for which structures have been solved have a naturally occurring zinc ion with either octahedral or square pyramidal coordination, i.e. purple acid phosphatase (Sträter *et al.*, 1995) and staphylococcal enterotoxin type A (Schad *et al.*, 1995). In purple acid phosphatase, the zinc ion is involved in an Fe(III)–Zn(II) active centre and has a distorted octahedral coordination. In the enterotoxin, the zinc is not involved in enzymatic activity, but is important for the binding of the protein to major histocompatibility complex class II molecules. In the structure of this enzyme, the zinc was replaced with $Cd^{2+}$ and the sixth zinc ligand (a water molecule) is only seen in one of the two molecules in the asymmetric unit. Only in glyoxalase I, however, is the octahedrally coordinated zinc playing a catalytic role in a single metal active centre. It has been suggested that an unusual coordination may explain why the zinc ion of glyoxalase I can be replaced, with essentially no reduction in turnover number, by $Mg^{2+}$, an ion which generally adopts an octahedral environment (Sellin *et al.*, 1983; Sellin and Mannervik, 1984).

In the crystal structure, the glutathione conjugate is bound immediately 'above' the zinc ion, at the entrance to the otherwise open β barrel (Figure 3). This places the sulfur atom of the glutathione 3.7 Å from the observed zinc coordinated water, with the sulfur, water and zinc atoms co-linear. Including a second water molecule as the sixth ligand would result in close contacts with the benzyl ring of the inhibitor as well as with the amido and carboxylate groups of residues Gln 33 and Glu 99.

### *Glutathione binding site*

The tripeptide glutathione conjugate is bound in an extended conformation. The interactions with the enzyme are markedly different from those seen in glutathione transferase A1-1, for example, where there are salt links and hydrogen bonds to the polar groups of all three residues of the tripeptide (Sinning *et al.*, 1993). In glyoxalase I, the only polar interactions with the protein involve the γ-glutamyl residue of glutathione, although at this position they are highly specific: the carboxylate group forms a salt link with the guanidino group of Arg 37 and the amide group of Asn 103 hydrogen bonds with both the carboxylate and the amino group of the γ-glutamate. Arg 122 is also within hydrogen bonding distance of the carboxylate group of the γ-glutamate. All other polar interactions are with water molecules. Additionally, the aromatic rings of residues Phe 67 and Phe 162 lie above, and in the plane of, the peptide linkages of the tripeptide. The electron density for the glycyl residue of the GSH is not so well formed, probably because of the lack of specific

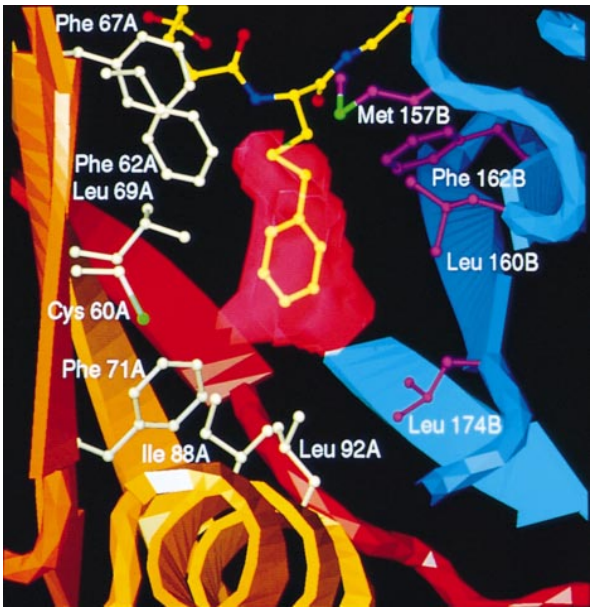


**Fig. 4.** The hydrophobic substrate binding pocket viewed from the side. The semi-transparent surface has been calculated with VOIDOO (Kleywegt and Jones, 1994a). The schematic representation of the backbone has been coloured as in Figure 1. The carbon atoms of the inhibitor and the two different subunits of the dimer have been coloured yellow, cream and magenta, respectively. The C-terminal helix which folds over the top of the inhibitor and the residues involved in zinc binding have been omitted for clarity. The side chains lining this cavity come from both monomers and are all hydrophobic (Met 157, Leu 160, Phe 162, Leu 174, Met 179, Met 183 from one monomer; Cys 60, Phe 62, Met 65, Phe 67 Leu 69, Phe 71, Ile 88, Leu 92 from the other), apart from residue Asn 32 which is located at the bottom. The figure was prepared in O (Jones and Kjeldgaard, 1991; Jones *et al.*, 1991).

interactions. As in alpha class glutathione transferase A1-1 (Sinning *et al.*, 1993), and in agreement with inhibitor binding studies (Vince and Wadd, 1969; Aronsson *et al.*, 1981), the benzyl group of the conjugate is located in a hydrophobic cavity. The volume of this cavity (~70 Å$^3$; see Materials and methods), situated at the dimer interface, is larger than that of the benzyl group which does not extend fully to the bottom (Figure 4). When a much larger substrate binds, such as the thiohemiacetal of *p*-phenylphenylglyoxal (Ridderström and Mannervik, 1996a), it is possible that the final three residues of the C-terminal helix could shift to accommodate it, since, from their associated electron density, these residues appear to be somewhat flexible.

### *Reaction mechanism*

Glyoxalase I carries out a simple isomerization reaction very efficiently, with the $k_{cat}/K_M$ value close to being diffusion limited (Marmstål *et al.*, 1979). The mechanism has been much discussed in the literature and appears to involve an enediol intermediate and a shielded proton transfer (see Figure 5). The similarities of such a mechanism to that proposed for TIM (Knowles, 1991) are obvious, and a comparison of the respective sequences of these two enzymes has led to the suggestion that a region around the conserved Glu 99 may be a counterpart to the catalytic loop seen in TIM, with Glu 99 acting as the essential base (Lan *et al.*, 1995). Mutating this residue, in the bacterial enzyme, to an aspartic acid does indeed result in the loss

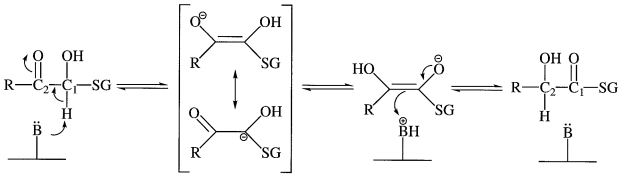

**Fig. 5.** Proposed reaction mechanism for glyoxalase I. A shielded base (B) is proposed to abstract the proton from the C1 atom of the hemithioacetal of glutathione and a 2-oxoaldehyde and then reprotonate at C2.

of enzymatic activity (Lan *et al.*, 1995). However, in the structure this residue coordinates the zinc ion and so its modification probably alters, and perhaps destroys, the zinc binding site. The mechanism proposed by Mannervik and co-workers involves a base extracting a proton from the C1 atom of the substrate, while the keto group hydrogen bonds to a zinc-bound water that acts as a Brønsted acid (Sellin *et al.*, 1982a,b). In the structure, however, all the residues in the vicinity of the C1 atom, apart from the zinc ligands, are hydrophobic and so there is no obvious candidate for a base. We are, therefore, forced to consider the zinc ligands as possible bases. Experiments on both yeast and rat glyoxalase I indicate the presence of dissociable groups with p$K_a$ values of 5 and 8.5 (Vander Jagt and Han, 1973; Vander Jagt, 1989) and that there is little variation in $k_{cat}$ in the pH range between 4.5 and 9. One would expect the p$K_a$ of the carboxylate ligands to be affected by their interaction with the zinc ion, but to what extent will depend on the net charge of the complex. Given that the net charge of the zinc–ligand complex is zero and the carboxylates are situated in a hydrophobic environment, one carboxylate may have a p$K_a$ value as high as 5. The p$K_a$ of the water molecule should also be modified by its interaction with the zinc ion. In carbonic anhydrase, for example, where the net charge on the active site zinc–ligand complex is +2, the p$K_a$ of the zinc-bound water molecule is 7.0 (Coleman, 1971). Because of the differences in net charge and coordination geometry between these two enzymes, we expect the p$K_a$ of the zinc-bound water in glyoxalase I to be higher. Preliminary modelling of both *R* and *S* enantiomers of a 2-oxoaldehyde thiohemiacetal substrate allows the placement of the C1-H group close to the bound water, with the aromatic/aliphatic group of the substrate positioned in the hydrophobic pocket. In this position, the carboxylate group of Glu 172 is also <4 Å from the C1 atom. Thus, from a structural point of view, either the water or the glutamate are in a position to abstract a proton from the C1 atom. The water molecule expected to occupy the sixth coordination position and Glu 99 may also play a role in the reaction mechanism by interacting with the carbonyl oxygen on C2. It would seem, therefore, that the reaction mechanism is rather more complicated than that shown in Figure 5 and investigations to elucidate this mechanism are being carried out using site-directed mutagenesis and structural analyses.

### *Sequence alignment*

An alignment of the sequences of the two domains based on their structural similarity shows that 13 residues are identical, out of 74 in domain 1 and out of 59 in domain 2 (see Figure 2B). The conserved residues include the

zinc ligands (Glu 99 and Glu 172) and three pairs of residues interacting with the inhibitor (Met 65, Met 157; Leu 69, Leu 160; Phe 71, Phe 162). It seems, therefore, that glyoxalase I has arisen by a gene duplication that resulted in the formation of the zinc binding and active sites. The other conserved residues are mainly involved in the core regions of the motif.

Seven glyoxalase I sequences have been reported: from human (Kim *et al.*, 1993; Ranganathan *et al.*, 1993; Ridderström and Mannervik, 1996a); two yeasts, *Saccharomyces cerevisae* (Gentles *et al.*, 1995; Inoue and Kimura, 1996) and *Schizosaccharomyces pombe* (Devlin *et al.*, 1995); a plant, *Solanum lycopersicum* (Espartero *et al.*, 1995); and sequences from the bacteria *Pseudomonas putida* (Lu *et al.*, 1994), *E.coli* (Daub *et al.*, 1996a) and *Salmonella typhimurium* (Daub *et al.*, 1996b). Whereas the human, bacterial and plant glyoxalase I enzymes are dimeric, the yeast enzymes are monomers of 32 and 37 kDa, respectively, with two copies of a segment equivalent to the monomer of the human protein (Ridderström and Mannervik, 1996b). This suggests that two gene duplication events occurred during the evolution of the yeast glyoxalase I.

The sequences are aligned in Figure 6A. It is apparent that the regions encoding the secondary structural elements within the βαβββ motif are fairly well conserved. On the other hand, not all the glyoxalase I enzymes have helices α3 or α5 which together make up the bottom of the barrel. This means that the shape of the active site will be different among the various enzymes. Looking at the conservation of selected amino acids, it can be seen that, apart from Arg 122, the residues involved in metal and glutathione binding are conserved throughout the known sequences. There are some conservative substitutions, however. The equivalent of Gln 33 in the human enzyme is a histidine in all the other sequences apart from tomato. That a histidine occurs at this position is not surprising if the gene duplication theory is to be believed, since the equivalent residue in domain 2 is also a histidine. Phe 67 is replaced by a tyrosine in both the *E.coli* and *S.typhimurium* enzymes. In the yeast sequences, all the residues that appear to be important in forming the active site are conserved in both the N- and C-terminal segments. It seems likely, therefore, that the folded protein monomers will mimic the dimer seen in the human enzyme, and give two similar, but not identical, active sites.

In addition to the known glyoxalase I sequences, a BLAST search (Altschul *et al.*, 1990), carried out at the Ecole Polytechnique Federale de Lausanne (EPFL), picked out five other sequences of proteins with unknown function that have high sequence similarity to human glyoxalase I (Figure 6A). These are from *Haemophilus influenzae* (Fleischmann *et al.*, 1995), *Vibrio parahaemolyticus* (McCarter, 1994), *Synechocystis* sp. (Kaneko *et al.*, 1995) and *Brassica oleracea* (Croy, 1996a,b). All these sequences contain the appropriate residues for binding the metal and glutathione, except for the genes from *B.oleracea*. The two sequences from *B.oleracea* are very similar (97% in the core region), but one is shorter than the other, missing 27 residues at the N-terminus (including residues involved in metal and GSH binding). As for the yeast enzyme, the sequences of the *B.oleracea* genes contain a duplication such that the N- and C-terminal halves can be aligned as separate units. In both *B.oleracea* genes, the residue corresponding to one of the zinc ligands in the human enzyme, Glu 172, is replaced by a valine. The *B.oleracea* enzymes may, therefore, have only one active site.

Apart from the residues making direct contacts with either the zinc or the glutathione, a third group of conserved residues help form the periphery of the active site. For example, the Cγ atom of Thr 101 is within van der Waals contact of the γ-glutamate side chain of the glutathione, while the Oγ hydroxyl interacts with the amine nitrogen of the glutathione cysteine residue via a water molecule. Similarly, a hydrogen bond network connects the hydroxyl of Tyr 114 to the amino nitrogen of the glutathione via the amide group of Asn 103. The side chains of Met 35 and Phe 71 both fill hydrophobic pockets beside metal binding ligands. Gly 125, immediately adjacent to ligand His 126, is also highly conserved. It adopts an α-helical conformation, but is placed in a β strand. This main-chain irregularity allows Phe 124 (always an aromatic) to interact with a 2-fold related copy of itself and His 126 to point towards the active site. Introducing a larger side chain at this position would result in a clash with Met 35. It is only replaced by an alanine in the C-terminal sequences from *B.oleracea* where the metal binding site may be lost.

A fourth group of conserved residues belong to the hydrophobic core between the two active sites. These include Leu 31, Thr 34, Leu 36, Val 38, Tyr 48, Met 54, Leu 98, Phe 124, Ile 127 and Tyr 169. The reverse turn between strands β7 and β8 (residues 165–169; see Figure 6B) is highly conserved. This is an Asx turn, a conformation that also shows a strong proline preference for the following residue. In glyoxalase I, Asp 165 is buried with one carboxylate oxygen interacting with three consecutive main-chain nitrogens (167–169), and the other oxygen within hydrogen bonding distance of the hydroxyl of conserved Tyr 48 and a buried water. The other conserved aspartyl (residue 167), on the other hand, is accessible to bulk solvent. Gly 53 and its counterpart in the second domain, Gly 145, occur at turns immediately after an α helix (Schellman, 1980). Asp 40 and Asp 133 are also conserved between the two domains, forming N-caps of helices α2 and α4, respectively.

We cannot be sure whether all of these proteins exhibit the same domain swapping that is observed in the human enzyme. At first sight, the interdomain region looks rather different among the sequences. However, the deletions in some of the enzymes correspond to extra loops in the human enzyme and so the other structures can be easily modelled. All sequences have glycines at position 105 and 117, and either a glycine or an alanine at position 123 where there are sharp turns in the protein chain. Most ambiguity occurs at residue 117 where the Cα separation between the corresponding residues of the two monomers is only 7.4 Å (see Figure 6B). This means that only minor adjustments are needed for the domain swapping to be removed. However, the conservation of Tyr 114, Gly 117, Asn 118 and Gly 123 suggests that the domains remain swapped in all these enzymes. Since the conservation is not complete, final proof requires further structural investigations.

### *Comparison with other known structures*

The domain topology that we observe in glyoxalase I is different from that seen in many of the other glutathione-

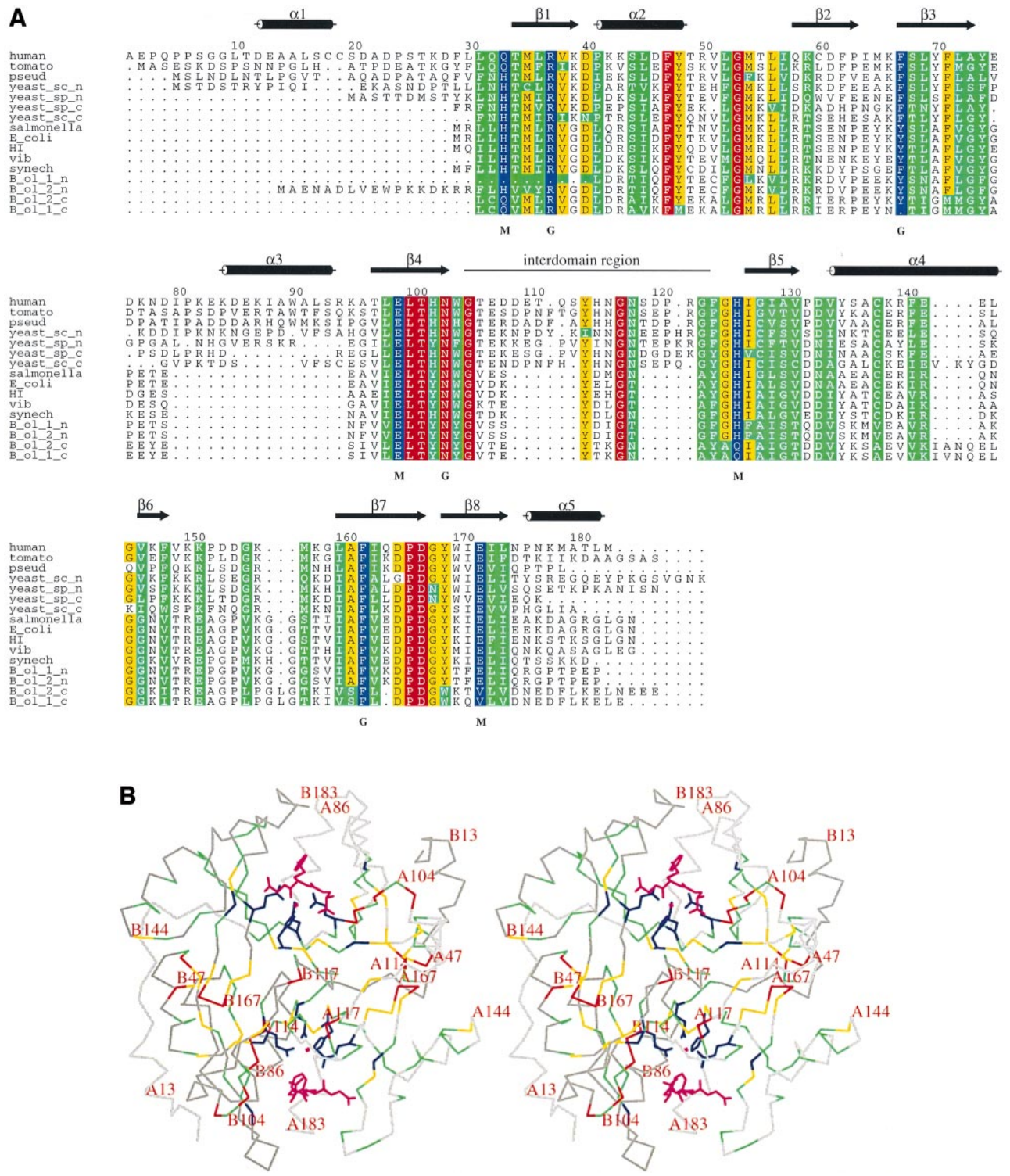


**Fig. 6.** (**A**) Sequence alignment of the glyoxalase I sequences. Human: *Homo sapiens* (Kim *et al.*, 1993; Ranganathan *et al.*, 1993; Ridderström and Mannervik, 1996a), tomato: *Solanum lycopersicum* (Espartero *et al.*, 1995), yeast_sc_n and yeast_sc_c: *Saccharomyces cerevisae* (Gentles *et al.*, 1995) N- and C-terminal portions respectively, yeast_sp_n and yeast_sp_c: *Schizosaccharomyces pombe* (Devlin *et al.*, 1995) N- and C-terminal portions, respectively, Salmonella: *Salmonella typhimurium* (Daub *et al.*, 1996b), E_coli: *Escherichia coli* (Daub *et al.*, 1996a), HI: *Haemophilus influenzae*, Swiss Prot. P44638 (Fleischmann *et al.*, 1995), Vib: *Vibrio parahaemolyticus*, Swiss Prot. P46235 (McCarter, 1994), synech: *Synechocystis* sp., EMBL D63999 (Kaneko *et al.*, 1995), B_ol_1_n, B_ol_1_c: *Brassica oleracea* (Croy, 1996a) N- and C-terminal halves, respectively, B_ol_2_n, B_ol_2_c: *Brassica oleracea* (Croy, 1996b) N- and C-terminal halves, respectively. The figure was prepared using the program ALSCRIPT (Barton, 1993) and the sequence alignment using the program MULTALIN (Corpet, 1988). The residues interacting with the metal or glutathione are marked in dark blue, those that are identical in all sequences in red, those in more than 14 out of 16 sequences in orange and those that are conserved but not identical in green. Conservation was calculated in ALSCRIPT using a conservation value of five. (**B**) Stereo diagram of the glyoxalase I dimer coloured according to residue conservation as above. The non-conserved residues of the A and B molecules are coloured light and dark grey, respectively.

**Table I.** Data collection and phasing statistics

| Data set | Apo | BGSH-L[a] | BGSH-H[a] | Pt[b] | IBGSH[c] |
|---|---|---|---|---|---|
| Cell dimensions (Å) | a = b = 68.3<br>c = 169.8 | a = b = 68.2<br>c = 169.8 | a = b = 68.0<br>c = 169.4 | a = b = 68.5<br>c = 168.9 | a = b = 68.4<br>c = 169.9 |
| Resolution range (Å) | 30–3.0 | 30–2.7 | 30–2.2 | 30–2.7 | 30–2.7 |
| Measured reflections | 82 009 | 102 266 | 118 633 | 70 410 | 121 555 |
| Unique reflections | 15 096 | 21 002 | 35 503 | 20 874 | 21 006 |
| Completeness (%) | 98.1 (83.3)[d] | 99.5 (95.7) | 91.3 (79.1) | 99.2 (92.6) | 99.3 (94.5) |
| $R_{merge}$[e] | 5.3 (10.1) | 6.2 (13.4) | 6.8 (24.8) | 6.0 (17.4) | 4.9 (13.5) |
| $<I/\mathrm{sig}I>$ | 25.6 (12.2) | 21.0 (9.7) | 17.8 (3.4) | 15.8 (4.9) | 26.6 (10.4) |
| $R_{iso}$[f] | | | | 21.3 (24.9) | 8.4 (10.1) |
| [g]Phasing power (acentric) | | | | 1.6–3 Å | 1.2–4.5 Å[g] |
| [h]$R_{cullis\ (acentric)}$ | | | | 0.78–3 Å | 0.78–4.5 Å |

[a]Crystals grown in the presence of 1 mM *S*-benzyl-glutathione (BGSH).
[b]Soaked crystal used to collect BGSH-L data for 16 h in 5 mM $PtNH_3CH_2CH_2Cl$.
[c]Soaked BGSH-L crystal in 2 mM *S-o*-iodo-benzyl-glutathione for 5 days.
[d]Numbers in parentheses are for the highest resolution bins.

[e]$R_{merge} = \sum_{hkl}\sum_{i}|<I(hkl)> - I(hkl)_i|/\sum_{hkl}\sum_{i}I(hkl)_i$.

[f]$R_{iso} = \sum||F_{PH}|-|F_P||/\sum|F_P|$ where $|F_{PH}|$ is the observed structure factor amplitude of the derivative and $|F_P|$ is the observed structure factor amplitude of the Apo data set.

[g]Phasing power = r.m.s. $(|F_H|/|F_{PH}-|F_P + F_H||)$.

[h]$R_{cullis} = \sum|F_{PH}-|F_P + F_H||/\sum|F_{PH}-F_P|$.

linked enzymes, such as glutathione transferase (Reinemer *et al.*, 1991; Sinning *et al.*, 1993). In these enzymes, the GSH binding domain is an α/β structure with a mixed four-stranded β sheet together with three α helices. Although this domain is also built up from a β sheet of four strands, its topology differs from that seen in the glyoxalase I domains. The glyoxalase I structure is, however, very similar to both the bleomycin resistance protein (BRP) (Dumas *et al.*, 1994) and the dihydroxybiphenyl dioxygenase (DHBD) (Han *et al.*, 1995; Senda *et al.*, 1996) (Figure 1). Like human glyoxalase I, each of these proteins is built up from four βαβββ domains, arranged in pairs to form an eight-stranded β sheet. Although the three proteins are functionally distinct, the substrate or antibiotic binding sites are all in spatially equivalent positions on the inner face of the β sheet. Differences in the overall shapes of these binding sites are caused by the extra helices in glyoxalase I, an extra strand in DHBD and a slight twisting of the domains with respect to one another in BRP. A comparison of the three proteins is interesting from an evolutionary perspective. Dumas *et al.* (1994) pointed out that in the dimeric BRP the first eight residues are mutually exchanged between the two monomers. In fact, BRP shows the same domain swapping that we observe in glyoxalase I, but because there is a slight twist between the domains the effect is not so evident.

In DHBD, on the other hand, the active site is formed in its entirety from two domains which are consecutive in sequence, i.e. there is no domain swapping (see Figure 1). DHBD is an octameric $Fe^{2+}$-dependent enzyme with one monomer equivalent to the complete dimer of glyoxalase I, but with only one active site. The similarity of this enzyme to glyoxalase I is emphasized by the fact that the three residues coordinating the iron are structurally equivalent to three of the four residues that bind the zinc in glyoxalase I. The two proteins, nevertheless, catalyse completely different reactions. The resemblance of DHBD and glyoxalase I extends to their molecular mass distributions. There are two classes of DHBD, one of ~21 kDa and the other of ~33 kDa. As for glyoxalase I, the smaller molecular mass protein has been proposed to dimerize to give a quaternary structure which mimics the subunit of the larger protein (Han *et al.*, 1995).

A detailed understanding of what is causing the swapping in glyoxalase I and BRP remains to be determined. It should be remembered, however, that in glyoxalase I some of the residues belonging to the interdomain region are conserved and appear to help form the active site. Since the Cα atoms of residue 114 of one monomer and 123 of the other are only 4.7 Å apart, it would be interesting to see whether by making a seven residue deletion the protein would fold without the domain swap.

## Materials and methods

### *Crystallization*

Recombinant protein was expressed and purified as described previously (Ridderström and Mannervik, 1996a). The sequence is the allelic variant containing Glu rather than Ala at position 110. Native crystals were grown in hanging drops with PEG 2000 monomethyl ether as precipitant. An equal volume of well liquor containing 25–30% w/v PEG, 50 mM MES (pH 5.8) and 0.1 M NaCl was mixed with 5 µl of a 12 mg/ml protein solution containing 1% 2-mercaptoethanol. Crystals containing *S*-benzyl-glutathione were prepared in the same way, but with the inclusion of the inhibitor to a final concentration of 1 mM in the drop. Crystals of dimensions ~0.3×0.3×0.3 mm appeared after about a week at 15°C.

### *Data collection and structure solution*

Data were recorded at room temperature on a Rigaku R-AXIS imaging plate mounted on a rotating anode source and integrated and scaled using the HKL suite (Otwinowski, 1993). Further processing was carried out using programs from the CCP4 package (Collaborative Computational Project Number 4, 1994). Data collection statistics can be seen in Table

I. The space group was determined to be either $P4_1$ or the enantiomorph $P4_3$ with two dimers in the asymmetric unit. The first platinum site was located using the program RSPS (Knight, 1989) from a difference Patterson calculated to 4.5 Å, between the BGSH-L and Pt data sets (see Table I). The program MLPHARE (Otwinowski, 1991) was then used to refine the heavy atom parameters and calculate phases to 4.5 Å. Since the IBGSH data set was more isomorphous to the Apo than to the BGSH-L data (see Table I), the Apo data were taken as the native in the heavy atom refinement and phasing calculations. Further platinum and iodine sites were located using difference Fourier maps. The initial MIR map, based on phases calculated to 3 Å (overall figure of merit: 0.38 acentric reflections; 0.67 centric reflections), showed defined solvent boundaries from which the two dimers of the asymmetric unit could be distinguished. A mask was created around one of the dimers and the map subjected to 10 cycles of 4-fold averaging in RAVE (Kleywegt and Jones, 1994b) making use of the proper symmetry between the monomers of each dimer and the improper symmetry between the dimers. The non-crystallographic symmetry operators were determined using the positions of the heavy atom sites and improved using the IMP program from the RAVE package. From the handedness of the helices, the space group was determined to be $P4_3$ rather than $P4_1$. The map was then subjected to a further 20 cycles of averaging against the slightly higher resolution 2.7 Å BGSH-L data.

### *Model building, refinement and analysis*

The model was built in O using skeletonized density, main and side chain databases and baton building methods (Jones and Kjeldgaard, 1991; Jones *et al.*, 1991). Refinement was carried out in X-PLOR (Brünger, 1992), initially against the 2.7 Å BGSH-L data, but in the final stages against the 2.2 Å BGSH-H data. Refinement involved cycles of simulated annealing using the slow-cool procedure (Brünger and Krukowski, 1990) interspersed with manual rebuilding into maps averaged using RAVE. All maps were calculated with a low-resolution cut-off of 15 Å. Strict non-crystallographic symmetry constraints were maintained at all times since relaxing these constraints resulted in no appreciable drop in R-free (based on 5% of the data selected in thin shells) and no significant difference in the resulting maps. Individual B-factors were refined with restraints between bonded atoms. The final R-factor is 21.1% and R-free 23.4%. Only 0.6% of residues are outside a stringent boundary Ramachandran plot (Kleywegt and Jones, 1996). The r.m.s.d. values from ideal bond angles, bond lengths and impropers (Engh and Huber, 1992) are 0.009 Å, 1.52° and 1.23°, respectively, and the r.m.s. B-value between bonded atoms is 2.0 $Å^2$. Structural superposition of the various molecules was carried out in O such that all matching Cα pairs were $<3.8$ Å apart after the superposition. The volume of the substrate binding pocket was calculated using the program VOIDOO (Kleywegt and Jones, 1994a) as the volume accessible to a probe of radius 1.2 Å. This calculation used a model containing all protein atoms, the zinc ion, the zinc-bound water and all atoms of the glutathione moiety apart from the cysteinyl side chain. The Dali program (Holm and Sander, 1993) was used to search the FSSP database version 1.0 (April 1, 1995) (Holm *et al.*, 1992; Holm and Sander, 1994) for structures with a similar fold to glyoxalase I. Maps calculated from the Apo data set showed significant electron density for a glutathione-derived ligand. This suggests that the hexyl glutathione that had been used to elute the protein from the affinity column during purification had not been completely removed by dialysis. No attempt was made, therefore, to compare the 'Apo' structure with the ligand-bound structure. The coordinates and structure factor amplitudes have been deposited in the Brookhaven Protein Data Bank with entry code Ijro VRML molecular images of glyoxalase I and of the complete electron density are available on http://alpha2.bmc.uu.se/vrml/glxI.

## Acknowledgements

We thank Marc Bergdoll for providing the coordinates of BRP. This work was supported by the Swedish Natural Science Research Council and the Carl Trygger Foundation. A.D.C. was supported by the Göran Gustafson Stiftelse.

## References

Altschul,S.F., Gish,W., Miller,W., Myers,E.W. and Lipman,D.J. (1990) Basic local alignment search tool. *J. Mol. Biol.*, **215**, 403–410.

Aronsson,A.-C., Marmstål,E. and Mannervik,B. (1978) Glyoxalase I, a zinc metalloenzyme of mammals and yeast. *Biochem. Biophys. Res. Commun.*, **81**, 1235–1240.

Aronsson,A.-C., Sellin,S., Tibbelin,G. and Mannervik,B. (1981) Probing the active site of glyoxalase I from human erythrocytes by use of the strong reversible inhibitor *S-p*-bromobenzylglutathione and metal substitutions. *Biochem. J.*, **197**, 67–75.

Barton,G.J. (1993) ALSCRIPT: a tool to format multiple sequence alignments. *Prot. Eng.*, **6**, 37–40.

Bennett,M.J., Schlunegger,M.P. and Eisenberg,D. (1995) 3D Domain swapping: A mechanism for oligomer assembly. *Protein Sci.*, **4**, 2455–2468.

Bock,C.W., Katz,A.K. and Glusker,J.P. (1995) Hydration of zinc ions: A comparison with magnesium and beryllium ions. *J. Am. Chem. Soc.*, **117**, 3754–3765.

Brünger,A. (1992) *X-PLOR Version 3.1: A System For Crystallography and NMR*. Yale University Press, New Haven, CT.

Brünger,A.T. and Krukowski,A. (1990) Slow-cooling protocols for crystallographic refinement by simulated annealing. *Acta Crystallogr.*, **A46**, 585–593.

Christianson,D.W. (1991) Structural biology of zinc. *Adv. Protein Chem.*, **42**, 281–355.

Coleman,J.E. (1971) Metal ions in enzymatic catalysis. *Prog. Biorg. Chem.*, **1**, 159–344.

Collaborative Computational Project Number 4 (1994) The CCP4 Suite: programs for protein crystallography. *Acta Crystallogr.*, **D50**, 760–763.

Corpet,F. (1988) Multiple sequence alignment with hierarchical clustering. *Nucleic Acids Res.*, **16**, 10881–10890.

Croy,R.D. (1996a) GenBank accession number Z74950.

Croy,R.D. (1996b) GenBank accession number Z74962.

Daub,E., Kinach,R., Miedema,D., Barnard,J.F.J., Clugston,S.L. and Honek,J.F. (1996a) *Escherichia coli* glyoxalase I. Genbank accession number U57363.

Daub,E., Kinach,R., Miedema,D., Barnard,J.F.J., Clugston,S.L. and Honek,J.F. (1996b) *Salmonella typhimurium* glyoxalase I. Genbank accession number U57364.

Devlin,K., Churcher,C.M., Barrell,B.G., Rajandream,M.A. and Walsh,S.V. (1995) Swiss Protein Bank accession number Q09751.

Dumas,P., Bergdoll,M., Cagnon,C. and Masson,J.-M. (1994) Crystal structure and site-directed mutagenesis of a bleomycin resistance protein and their significance for drug sequestering. *EMBO J.*, 2483–2492.

Engh,R.A. and Huber,R. (1992) Accurate bond and angle parameters for X-ray protein structure refinement. *Acta Crystallogr.*, **A47**, 392–400.

Espartero,J., Sánchez-Aguayo,I. and Pardo,J.M. (1995) Molecular characterization of glyoxalase-I from a higher plant; upregulation by stress. *Plant Mol. Biol.*, **29**, 1223–1233.

Fleischmann,R.D. *et al.* (1995) Whole-genome random sequencing and assembly of *Haemophilus influenzae* Rd. *Science*, **269**, 496–512.

Garcia-Iniguez,L., Powers,L., Chance,B., Sellin,S., Mannervik,B. and Mildvan,A.S. (1984) X-ray absorption studies of the $Zn^{2+}$ site of glyoxalase I. *Biochemistry*, **23**, 685–689.

Gentles,S., Bowman,S., Barrell,B.G., Rajandream,M.A. and Walsh,S.V. (1995) Swiss Protein Bank accession number P50107.

Gillespie,E. (1979) Effects of S-lactoylglutathione and inhibitors of glyoxalase I on histamine release from human leukocytes. *Nature*, **277**, 135–137.

Han,S., Eltis,L.D., Timmis,K.N., Muchmore,S.W. and Bolin,J.T. (1995) Crystal structure of the biphenyl-cleaving estradiol dioxygenase from a PCB-degrading pseudomonad. *Science*, **270**, 976–980.

Holm,L. and Sander,C. (1993) Protein structure comparison by alignment of distance matrices. *J. Mol. Biol.*, **233**, 123–138.

Holm,L. and Sander,C. (1994) The FSSP database of structurally aligned protein fold families. *Nucleic Acids Res*, **22**, 3600–3609.

Holm,L., Ouzounis,C., Sander,C., Tuparev,G. and Vriend,G. (1992) A database of protein structure families with common folding motifs. *Protein Sci.*, **1**, 1691–1698.

Inoue,Y. and Kimura,A. (1996) Identification of the structural gene for glyoxalase I from *Saccharomyces cerevisiae*. *J. Biol. Chem.*, **271**, 25958–25965.

Jones,T.A. and Kjeldgaard,M. (1991) *O, The Manual*. Uppsala, Sweden.

Jones,T.A., Zou,J.Y., Cowan,S.W. and Kjeldgaard,M. (1991) Improved methods for building protein models in electron density maps and the location of errors in these models. *Acta Crystallogr.*, **A47**, 110–119.

Kaneko,T., Tanaka,A., Sato,S., Kotani,H., Sazuka,T., Miyajima,N., Sugiura,M. and Tabata,S. (1995) Sequence analysis of the genome of the unicellular cyanobacterium *Synechocystis sp.* strain PCC6803. I.

Sequence features in the 1 Mb region from map positions 64% to 92% of the genome. *DNA Res.*, **2**, 153–166.
Kim,N.-S., Umezawa,Y., Ohmura,S. and Kato,S. (1993) Human glyoxalase I: cDNA cloning, expression and sequence similarity to glyoxalase I from *Pseudomonas putida*. *J. Biol. Chem.*, **268**, 11217–11221.
Kleywegt,G. and Jones,T. (1994a) Detection, delineation, measurement and display of cavities in macromolecular structures. *Acta Crystallogr.*, **D50**, 178–185.
Kleywegt,G. and Jones,T. (1994b) Halloween... masks and bones. In Bailey,S., Hubbard,R. and Waller,D. (eds), *From First Map to Final Model*. EPSRC, Daresbury Laboratory, Daresbury, UK, pp. 59–66.
Kleywegt,G. and Jones,T. (1996) Phi/Psi-chology: Ramachandran revisited. *Structure*, **4** 1395–1400.
Knight,S. (1989) Ribulose 1,5-bisphosphate carboxylase/oxygenase—a structural study. PhD Thesis, Swedish University of Agricultural Sciences, Uppsala, Sweden.
Knowles,J.R. (1991) Enzyme catalysis: not different, just better. *Nature*, **350**, 121–124.
Kraulis,P.J. (1991) MOLSCRIPT: a program to produce both detailed and schematic plots of protein structures. *J. Appl. Crysallogr.*, **24**, 946–950.
Lan,Y., Lu,T., Lovett,P.S. and Creighton,D.J. (1995) Evidence for a (triosephosphate isomerase-like) 'catalytic loop' near the active site of glyoxalase I. *J. Biol. Chem.*, **270**, 12957–12960.
Lu,T., Creighton,D.J., Antoine,M., Fenselau,C. and Lovett,P.S. (1994) The gene encoding glyoxalase I from *Pseudomonas putida*: cloning, overexpression, and sequence comparisons with human glyoxalase I. *Gene*, **150**, 93–96.
Mannervik,B. (1980) Glyoxalase I. In Jakoby,W.B. (ed.), *Enzymatic Basis of Detoxication*. Academic Press, New York, Vol. 2, pp. 263–273.
Marmstål,E., Aronsson,A.-C. and Mannervik,B. (1979) Comparison of glyoxalase I purified from yeast (*Saccharomyces cerevisiae*) with the enzyme from mammalian sources. *Biochem. J.*, **183**, 23–30.
McCarter,L.L. (1994) MotY, a component of the sodium-type flagellar motor. *J. Bacteriol.*, **176**, 4219–4225.
Otwinowski,Z. (1991) Maximum likelihood refinement of heavy atom parameters. In Evans,P. and Leslie,A. (eds), *Isomorphous Replacement and Anomalous Scattering*. SERC Daresbury Laboratory, UK, pp. 80–85.
Otwinowski,Z. (1993) Oscillation data reduction program. In Sawyer,L., Isaacs,N. and Bailey,S. (eds), *Data Collection and Processing*. SERC Daresbury Laboratory, UK, pp. 56–63.
Ranganathan,S., Walsh,E.S., Godwin,A.K. and Tew,K.D. (1993) Cloning and characterization of human colon glyoxalase-I. *J. Biol. Chem.*, **268**, 5661–5667.
Reinemer,P., Dirr,H.W., Ladenstein,R., Schaffer,J., Gallay,O. and Huber,R. (1991) The three-dimensional structure of class-pi glutathione S-transferase in complex with glutathione sulfonate at 2.3 Å resolution. *EMBO J.*, **10**, 1997–2005.
Richard,J.P. (1991) Kinetic parameters for the elimination reaction catalyzed by triosephosphate isomerase and an estimation of the reaction's physiological significance. *Biochemistry*, **30**, 4581–4585.
Ridderström,M. and Mannervik,B. (1996a) Optimized heterologous expression of the human zinc enzyme glyoxalase I. *Biochem. J.*, **314**, 463–467.
Ridderström,M. and Mannervik,B. (1996b) The primary structure of monomeric yeast glyoxalase I indicates a gene duplication resulting in two similar segments homologous with the subunit of dimeric human glyoxalase I. *Biochem. J.*, **316**, 1005–1006.
Schad,E.M., Zaitseva,I., Zaitsev,V.N., Dohlsten,M., Kalland,T., Schlievert,P.M., Ohlendorf,D.H. and Svensson,L.A. (1995) Crystal structure of the superantigen staphylococcal enterotoxin type A. *EMBO J.*, **14**, 3292–3301.
Schellman,C. (1980) In Jaencke,R. (ed.), *Protein Folding*. Elsevier, Amsterdam, pp. 53–62.
Sellin,S. and Mannervik,B. (1984) Metal dissociation constants for glyoxalase I reconstituted with $Zn^{2+}$, $Co^{2+}$, $Mn^{2+}$, and $Mg^{2+}$. *J. Biol. Chem.*, **259**, 11426–11429.
Sellin,S., Eriksson,L.E.G. and Mannervik,B. (1982a) Fluorescence and nuclear relaxation enhancement studies of the binding of glutathione derivatives to manganese-reconstituted glyoxalase I from human erythrocytes. A model for the catalytic mechanism of the enzyme involving a hydrated metal ion. *Biochemistry*, **21**, 4850–4857.
Sellin,S., Rosevear,P.R., Mannervik,B. and Mildvan,A.S. (1982b) Nuclear relaxation studies of the role of the essential metal in glyoxalase I. *J. Biol. Chem.*, **257**, 10023–10029.
Sellin,S., Eriksson,L.E.G., Aronsson,A.-C. and Mannervik,B. (1983) Octahedral metal coordination in the active site of glyoxalase I as evidenced by the properties of Co(II)-glyoxalase I. *J. Biol. Chem.*, **258**, 2091–2093.
Sellin,S., Eriksson,L.E.G. and Mannervik,B. (1987) Electron paramagnetic resonance study of the active site of copper-substituted human glyoxalase I. *Biochemistry*, **26**, 6779–6784.
Senda,T., Sugiyama,K., Narita,H., Yamamoto,T., Kimbara,K., Fukuda,M., Sato,M., Yano,K. and Mitsui,Y. (1996) Three-dimensional structures of free form and two substrate complexes of an estradiol ring-cleavage type dioxygenase, the BphC enzyme from *Pseudomonas* sp. strain KKS102. *J. Mol. Biol.*, **255**, 735–752.
Sinning,I. *et al*. (1993) Structure determination and refinement of human alpha class glutathione transferase A1-1, and a comparison with the mu and pi class enzymes. *J. Mol. Biol.*, **232**, 192–212.
Sträter,N., Klabunde,T., Tucker,P., Witzel,H. and Krebs,B. (1995) Crystal structure of a purple acid phosphatase containing a dinuclear Fe(III)-Zn(II) active site. *Science*, **268**, 1489–1492.
Szent-Györgyi,A. (1965) Cell division and cancer. *Science*, **149**, 34–37.
Thornalley,P.J. (1990) The glyoxalase system: new developments towards functional characterization of a metabolic pathway fundamental to biological life. *Biochem. J.*, **269**, 1–11.
Thornalley,P.J. (1993) The glyoxalase system in health and disease. *Mol. Aspects Med.*, **14**, 287–371.
Uotila,L. and Koivusalo,M. (1975) Purification and properties of glyoxalase I from sheep liver. *Eur. J. Biochem.*, **52**, 493–503.
Vander Jagt,D.L. (1989) The glyoxalase system. In Dolphin,D., Poulson,R. and Avramovic,O. (eds), *Coenzymes and Cofactors*. John Wiley and Sons, New York, Vol. 3A, pp. 597–641.
Vander Jagt,D.L. and Han,L.-P.B. (1973) Deuterium isotope effects and chemically modified coenzymes as mechanism probes of yeast glyoxalase-I. *Biochemistry*, **12**, 5161–5167.
Vince,R. and Wadd,W.B. (1969) Glyoxalase inhibitors as potential anticancer agents. *Biochem. Biophys. Res. Commun.*, **35**, 593–598.

*Received on December 12, 1996; revised on February 28, 1997*